AJNR

Radiologic Findings in Two Cases of Acute Schmörl's Nodes

Elisenda Grivé, Alex Rovira, Jaume Capellades, Antoni Rivas and Salvador Pedraza

Radiologic Findings in Two Cases of Acute Schmörl's Nodes

Elisenda Grivé, Alex Rovira, Jaume Capellades, Antoni Rivas, and Salvador Pedraza

Summary: We describe two cases of atypical acute Schmörl's nodes, one benign, the other on a tumoral vertebra. In both cases, MR imaging showed a decreased vertebral T1 signal and a slightly increased T2 signal. These signal intensities are indistinguishable from tumoral disease or inflammatory lesions. The identification of endplate defects or intranuclear cleft bending of the disk by either CT or MR may be helpful for the correct diagnosis of acute Schmörl's nodes.

Schmörl's nodes, cartilaginous nodes representing vertical disk prolapses through areas of weakness in the vertebral endplate, are observed with a high incidence on vertebral MR exams. Disruption of the cartilaginous plate can be produced by any disorder that weakens either the plate itself or the subchondral bone of the vertebral body, allowing herniation of disk material into the spongiosa. This disruption may be accentuated by obvious or occult trauma (1). MR imaging usually shows the contour defect and disk material in the vertebral endplate clearly; however, when the Schmörl's node is recent, it can be difficult to differentiate benign degenerative bone disease from malignant infiltration or infection. Our report describes MR and CT features in two patients with recently formed Schmörl's nodes, one benign, the other on a tumoral vertebra. Follow-up exams and vertebral biopsy were necessary to confirm the diagnosis.

Case Reports

Case 1 (Fig 1)

A 68-year-old woman was admitted to our hospital with symptoms of acute back pain without sciatica, which had appeared 15 days before and was related to a dorsolumbar flexion injury. She had a long history of dull low-back pain related to an L5–S1 spondylolisthesis. The neurologic examination and routine laboratory results were normal. Plain films of the dorsal and lumbar spine showed no abnormalities, except for the previously diagnosed spondylolistesis. An MR study performed 2 weeks later disclosed a diffuse, homogeneous, low signal in-

tensity in the T11 vertebral body on T1-weighted images, and a slight increase in signal intensity near the inferior endplate on T2-weighted images. Technetium bone scintigraphy 6 days later showed a focal high uptake over the T11 vertebral body. Fourteen days later, a CT study showed a radiolucent lesion surrounding a dense central area on the lower portion of T11. Based on these observations, the differential diagnosis included primary and metastasic bone tumor; however, a CT-guided percutaneous biopsy was negative for malignancy or infection. Three months later, the lesion was diagnosed as a Schmörl's node with central degenerative disk calcification after follow-up MR and CT. MR showed important reductions in the signal intensity alterations and some irregularity of the inferior endplate. Reformatted sagittal and coronal CT images revealed an irregular bony defect in the lower left portion of the vertebra, with disruption of the inferior endplate and disk calcification that extended into the bony defect. At 1-year follow-up, MR images depicted a typical Schmörl's node; ie, a bony defect in the vertebral endplate without signal-intensity alterations. The patient's back pain gradually diminished, with rest alone, 2 months after the onset of symptoms. At 1-year follow-up, she was symptom-free.

Case 2 (Fig 2)

A 38-year-old man was admitted to our hospital with a 6-week history of acute lumbar pain related to physical exertion that was relieved by rest. The physical and neurologic examinations were normal. Laboratory results were normal, except for the presence of a monoclonal immunoglobulin (IgG kappa) that initially was considered to be nonspecific. The initial plain film of the lumbar spine was normal, but CT study disclosed a radiolucent lesion on the L3 vertebral body without peripheral sclerosis. Technetium bone scintigraphy was negative. An MR study showed a low signal intensity that diffusely affected the L3 vertebral body, except for the anterior margin, on the T1-weighted images; the T2-weighted images showed a nodular hyperintensity on the posterior half of the vertebral body. The intranuclear cleft on the L2–L3 and L3–L4 disks had an unusual appearance, bending toward the L3 vertebral body. The contrast-enhanced T1-weighted images revealed two large intrabody herniations in which there was no enhancement in the two endplates, whereas the rest of the vertebra enhanced homogeneously. The diagnosis of acute Schmörl's nodes with surrounding inflammatory changes in the vertebral body was made on the basis of the MR appearance of the endplate defects. Follow-up MR imaging was done at 3 months, because the finding of two large Schmörl's nodes in the same vertebra related only by physical exertion was exceptional. The MR study showed an infiltrating lesion in the right posterior portion of the L3 vertebral body, the structure containing the two Schmörl's nodes. This lesion was the cause of the vertebra's fragility. A new technetium bone scintigraphy was again negative. CT-guided puncture disclosed the presence of a plasmacytoma, and the patient began radiation therapy.

Discussion

Schmörl's nodes are intraspongious herniations of intervertebral disk material through areas of
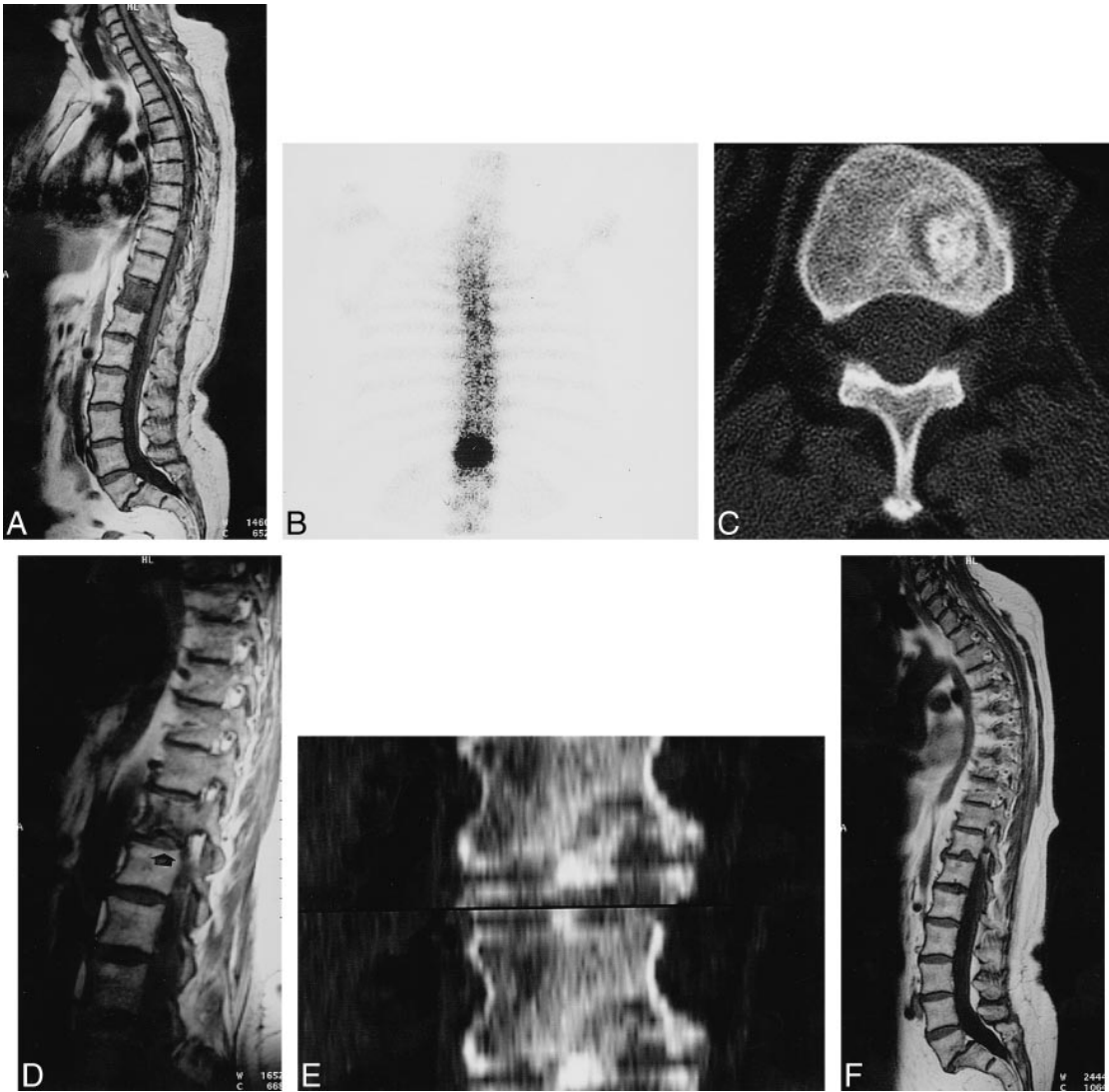
FIG 1. A 68-year-old woman with acute back pain of 15-day duration. Schmörl's node formation with herniation of calcified disk.

A, T1-weighted image spin-echo (600/15 [TR/TE]) shows diffuse low signal intensity in the T11 vertebral body and spondylolisthesis of L5–S1. T2-weighted spin-echo image (2200/80) shows only slight increase in signal intensity near inferior endplate (*arrow*).

B, Increased uptake on bone scintigraphy over T11 vertebra 6 days later.

C, CT scan depicts a radiolucent lesion in lower portion of T11 with central dense bone 14 days later.

D, Small defect (*arrow*) in inferior vertebral endplate of T11 and decrease in vertebral hypointensity on T1-weighted spin-echo image (500/15) 3 months later.

E, CT coronal reformatted images. Disk calcification herniating through vertebral bony defect.

F, T1-weighted spin-echo image (460/17) and T2-weighted spin-echo image (5000/112) (*arrow*) show a typical Schmörl's node at 1-year follow-up.

weakness in the endplate. The endplate defect may occur during development (through the vascular channels, through the region of the regressed chorda dorsalis, or through ossification gaps in the first and second decades of life), or may occur because of a weakening of the cartilaginous endplate or the subcondral bone by Scheuermann's disease, infection, metabolic disorders, neoplasms, degenerative disease, or traumatic lesions caused by compressive vertebral loads (1). The weakened endplate area has less resistance to the expansive pressure of the adjacent nucleus pulposus. The pressure decreases with age, and this accounts for the fact that Schmörl's node formation occurs more rapidly in younger persons. In a young individual, traumatic lesions are the common cause of focal endplate herniations, which only develop vertically because the annulus fibrosus is intact. After the third or fourth decade of life, herniations occur more gradually, often through disrupted portions of the degenerated cartilaginous plate, and in most cases they are associated with transverse disk herniation (1–3). Schmörl's nodes are commonly seen at radiographic examination or autopsy. Their incidence increases with age and they are more common in men than in women.

Characteristically, most Schmörl's nodes involve the inferior endplate adjacent to the nucleus pul-
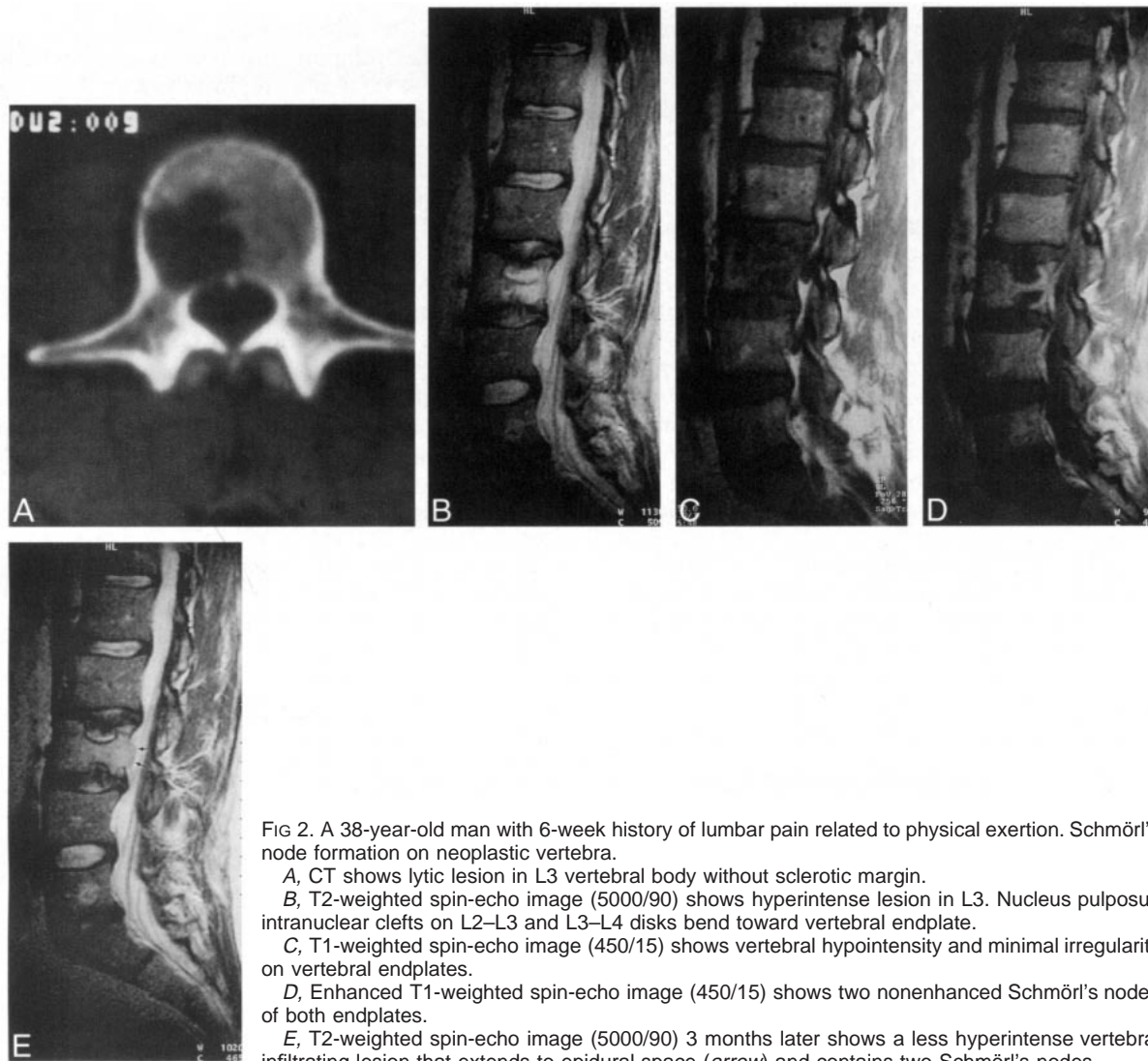
FIG 2. A 38-year-old man with 6-week history of lumbar pain related to physical exertion. Schmörl's node formation on neoplastic vertebra.

A, CT shows lytic lesion in L3 vertebral body without sclerotic margin.

B, T2-weighted spin-echo image (5000/90) shows hyperintense lesion in L3. Nucleus pulposus intranuclear clefts on L2–L3 and L3–L4 disks bend toward vertebral endplate.

C, T1-weighted spin-echo image (450/15) shows vertebral hypointensity and minimal irregularity on vertebral endplates.

D, Enhanced T1-weighted spin-echo image (450/15) shows two nonenhanced Schmörl's nodes of both endplates.

E, T2-weighted spin-echo image (5000/90) 3 months later shows a less hyperintense vertebral infiltrating lesion that extends to epidural space (*arrow*) and contains two Schmörl's nodes.

posus in the lower thoracic and upper lumbar spine (1, 2, 4). Pathologically, Schmörl's nodes represent the nucleus pulposus with degenerative or inflammatory changes and a confined sclerotic response in the adjacent vertebral spongiosa. This response has been thought to reflect reactive changes caused by repeated pressure, leading to trabecular condensation and thickening. After herniation into the trabecular bone, the avascular nucleus pulposus material can become vascularized. Calcification and ossification of the herniated disk may be noted 1, 5–8).

Regardless of the specific etiology, Schmörl's nodes are typically seen on plain film and CT scans as radiolucent lesions of varying size contained within the vertebral body at the endplate and are surrounded by a sclerotic margin that in extreme cases may involve most of the vertebral body (1). As occurred in case 1 (Fig 1), intravertebral herniation of a degenerated disk may lead to a calcification in an intraosseous location within the displaced disk material (8, 9). MR images show the herniated fragment of the nucleous pulposus inside the vertebral endplate, which leads to decreased width of the intervertebral disk space. Diagnosis of Schmörl's nodes is usually established after late changes have occurred and become visible on plain radiographs or CT scans.

In the acute stage, Schmörl's nodes are difficult to diagnose and even to detect, because sclerosis around the margin of the herniation has not had time to develop. MR studies, 2D reformatted CT images, tomography, and diskography are aids to early diagnosis (3, 8–11). Occasionally, serial plain radiographs show movement of a disk calcification to an intravertebral location (9). Schmörl's node formation, as demonstrated in case 1, is the healing process of an intraosseous fracture, with inflammation and edema that decreases progressively (3, 11, 12). MR imaging is the most sensitive noninvasive procedure for imaging acute-stage Schmörl's nodes. MR can show loss of signal intensity in the affected intervertebral disk space, the herniated fragment of the nucleous pulposus in some cases,

and signal changes in the underlying cancellous bone of the vertebral body, with low signal intensity on T1-weighted images and high signal intensity on T2-weighted images. These features may simulate a tumoral or inflammatory etiology, but they decrease in 3 to 12 months (9–13). Serial changes on CT scans reveal the progressive (3–24 months) thickening of the bony reaction around the lesion (11). Focal uptake has been reported on technetium bone mineral scanning, generally in the acute stage of symptomatic Schmörl's nodes, which normalizes some months after onset (3, 6, 8, 9, 11, 14). There is, however, a reported case of focal uptake in the absence of symptoms (15) and an acute, symptomatic Schmörl's nodes with normal bone scans (10, 13). In case 2, bone scintigraphy showed no increased uptake, as often happens in multiple myeloma or plasmacytoma because of the relative absence of reactive osteogenesis.

Although Schmörl's nodes are generally believed to be asymptomatic and have been found by MR imaging in 19% of people without back pain (4), they are more often seen in patients with lumbar symptoms (2) associated with degenerative changes at the diskcovertebral junction. Moreover, several reports have shown that Schmörl's nodes are of themselves related to back pain, which is most frequently located in the thoracolumbar spine (2, 3, 6–13).

Symptomatic cervical Schmörl's nodes has also been described (6). It appears that recent nodes, especially in young people with well-hydrated nucleus pulposus, are more painful (2, 3, 6, 9, 11–13). In symptomatic cases, the vertebral body marrow surrounding the node is generally seen as low signal intensity on T1-weighted images and high signal intensity on T2-weighted images. These features indicate the presence of an inflammatory bony response to the intraosseous fracture and intraspongious disk herniation, showing edema and acute and chronic inflammatory cells on histologic examination (6, 12). Stäbler et al (7) found that bone marrow reaction and clinical symptoms are significantly more frequent in large rather than in small Schmörl's nodes. Degenerative changes in the intravertebral herniation and vertebral body sclerosis can be painful; however, inflammatory bony changes are probably the main origin of the pain with Schmörl's nodes. In asymptomatic individuals, vertebral bone marrow MR signal changes are rarely seen. In conservatively treated symptomatic Schmörl's nodes, low-back pain gradually diminished and disappeared after 4 or 5 months (11–13). It is likely that symptomatic Schmörl's nodes arise from recent intraosseous fractures that become asymptomatic after resolution of the inflammation, as occurs with old vertebral compression fractures.

On plain-film or CT studies, the presence of a recent Schmörl's node may not be apparent; the findings may be interpreted as an osteolytic vertebral lesion, or, if the herniated disk is calcified, it may even be identified as an osteoblastic lesion. Moreover, early MR or scintigraphy findings are not specific, so differentiation from malignant disease or other inflammatory lesions can be difficult (8, 11, 12–15). Some reported cases have been highly suggestive of bone neoplasm on imaging studies, but after evolution or on histopathologic examination, the diagnosis was found to be Schmörl's nodes (8, 11). In light of these diagnostic difficulties, our experience has shown that it is of the utmost importance to look for the characteristic morphology of the endplate defect. Gd-DTPA–enhanced MR imaging was helpful in case 2 (Fig 2D), and in case 1, 2D reformatted CT (Fig 1E) enabled identification of the vertebral defect and differentiation of the calcified herniation from a tumoral lesion. Intranuclear cleft bending of the disk also suggested intravertebral disk herniation in case 2 (Fig 2B).

Neoplastic processes weaken the structural integrity of the supporting cancellous bone, making Schmörl's node formation more likely. Generally, metastatic or primary tumors of the spine do not produce significant alterations in the intervertebral disk, but when there is disruption of the endplate, they can mimic primary subcondral degenerative changes in the spine (1). Radiographic examination can disclose a Schmörl's node hiding a tumoral lesion (14), as in case 2 (Fig 2).

In conclusion, great care must be taken in interpreting MR signal intensity changes of the vertebral bodies. Recently formed Schmörl nodes can show signal intensities that are indistinguishable from tumoral disease or other inflammatory lesions, and tumoral infiltration can lead to cartilaginous node formation that mimics degenerative changes. Scintigraphy and axial CT sections may also be confusing in acute cases. If, however, the radiologist is aware of the morphologic characteristics of the endplate defect and adjacent disk, MR imaging is usually sufficient for reliable differentiation between degenerative bone disease and malignant infiltration or infection. Contrast-enhanced MR and 2D CT reformations can be helpful for distinguishing Schmörl's node from malignant disease in equivocal cases. The MR finding of intranuclear cleft bending of the disk may be helpful for identifying large, acute Schmörl's nodes. Conservative treatment should be the first choice in symptomatic Schmörl's nodes. If, however, the diagnosis is not clear in the first study, as in case 1, or nodal characteristics are atypical, as in case 2, a follow-up to discover the natural course of acute intravertebral herniation is essential.

Acknowledgments

References

1. Resnick D, Niwayama G. **Intravertebral disk herniations: Cartilaginous (Schmorl's) nodes.** *Radiology* 1978;126:57–65

2. Hamanishi C, Kawabata T, Yosii T, Tanaka S. **Schmorl's nodes on magnetic resonance imaging. Their incidence and clinical relevance.** *Spine* 1994;19:450–453
3. Mc Call IW, Park WM, O' Brien JP, Seal V. **Acute traumatic intraosseous disc herniation.** *Spine* 1985;10:134–137
4. Jensen MC, Brant-Zawadski MN, Obuchowski N, Modic MT, Malkasian D, Ross JS. **Magnetic Resonance Imaging of the lumbar spine in people without back pain.** *N Engl J Med* 1994;331:69–73
5. Mc Fadden KD, Taylor JR. **End-plate lesions of the lumbar spine.** *Spine* 1989;14:867–869
6. Lipson SJ, Fox DA, Sosman JL. **Symptomatic intravertebral disc herniation (Schmorl's node) in the cervical spine.** *Ann Rheum Dis* 1985;44:857–859
7. Stäbler A, Bellan M, Weiss M, Gärtner C, Brossmann J, Reiser MF. **MR imaging of enhancing intraosseous disc herniation (Schmörl's nodes).** *AJR Am J Roentgenol* 1997;168:933–938
8. Smith DM. **Acute back pain associated with a calcified Scmörl's node.** *Clin Orthop* 1976;117:193–196
9. Seymour R, Williams L.A, Rees J.I, Lyons K, Lloyd DCF. **Magnetic resonance imaging of acute intraosseous disc herniation.** *Clin Radiol* 1998;53:363–368
10. Kornberg M. **MRI diagnosis of traumatic Schmorl's node.** *Spine* 1988;13:934–935
11. Takahashi K, Takata K. **A large painful Schmorl's Node: a case report.** *J Spinal Disord* 1994;7:56–59
12. Takahashi K, Miyakazi T, Ohnari H, Takino T, Tomita K. **Schmorl's nodes and low back pain. Analysis of MRI findings in symptomatic and asymptomatic individuals.** *Eur Spine J* 1995;4:56–59
13. Walters G, Coumas JM, Akins CM, Ragland RL. **MRI of acute symptomatic Schmorl's node formation.** *Pediatr Emerg Care* 1991;7:294–296
14. Mc Lain R, Weinstein JN. **An unusual presentation of a Schmorl's node. Report of a case.** *Spine* 1990;15:247–250
15. Kagen S, Rafii M, Kramer EL. **Focal uptake on bone imaging in an asymptomatic Schmorl's node.** *Clin Nucl Med* 1988;13:615–616